In-vivo Measurement of Sound-induced Motions in the Gerbil Cochlea

by

Shirin Farrahi

BASc, Simon Fraser University (2007)

Submitted to the Department of Electrical Engineering and Computer Science
in partial fulfillment of the requirements for the degree of

Master of Science in Electrical Engineering

at the

MASSACHUSETTS INSTITUTE OF TECHNOLOGY

February 2010

Author .....
Department of Electrical Engineering and Computer Science
January 15, 2010

Certified by .....
Dennis M. Freeman
Professor
Thesis Supervisor

Accepted by .....
Terry P. Orlando
Chairman, Department Committee on Graduate Theses

In-vivo Measurement of Sound-induced Motions in the Gerbil Cochlea

by

Shirin Farrahi

Submitted to the Department of Electrical Engineering and Computer Science
on January 15, 2010, in partial fulfillment of the
requirements for the degree of
Master of Science in Electrical Engineering

Abstract

We developed methods to measure sound-induced motions in a live mammalian cochlea using a laser Doppler velocimeter (LDV). We measured the basilar membrane (BM) in the Mongolian gerbil at a distance of roughly 1.5 mm from the extreme base and found a best frequency (BF) of roughly 35 kHz. We chose the base to gain access through the round window membrane (RWM) to minimize the need for invasive surgery. Post-mortem measurements showed a 20dB drop in sensitivity as well as a half-octave drop in BF. The post-mortem phase led the in vivo phase below the BF and lagged the in vivo phase above the BF. These features of the post-mortem response agree with those seen by Overstreet [10] in the base of the gerbil cochlea. To look for evidence of radial modes in the BM, we measured points along the radius of the BM both in vivo and post-mortem. In the in vivo case, we found slightly sharper tuning in the center of the BM than on the edge but similar phase excursions. In the post-mortem case, we found similar bandwidths and phase excursions along the radius of the BM. Since in vivo measurements along the radius of the BM were only collected in one animal, we cannot yet conclude that there are multiple radial modes in the gerbil BM. In addition, our in vivo preparation was relatively insensitive as evidenced by compound action potential (CAP) thresholds greater than 80dB SPL in the region of interest. We identified the removal of the RWM as the cause for elevated CAP thresholds by comparing the CAP thresholds before and after removing the RWM to drop beads on the BM as essential reflective targets. Previous studies also suggest that large CAP threshold increases are common in the gerbil base ([10], [6]). Similar techniques have led to greater success in larger mammals; however, we hope to apply the lessons learned from measuring the in vivo gerbil cochlea to mice, the only species that would allow us to determine the micromechanical changes underlying genetic hearing disorders.

Thesis Supervisor: Dennis M. Freeman
Title: Professor

Acknowledgments

I would like to first thank my advisor, Prof. Dennis Freeman who pushed me to succeed on this project and taught me the keys to a rigorous scientific method. Secondly, Scott Page was a tremendous help both in teaching me to perform surgery on gerbils and for his technical prowess in programming and helping to design the data acquisition system. A.J. Aranyosi and Roozbeh Ghaffari were also great sources of technical assistance throughout this study. I'd like to thank Micheal Ravicz for taking time out of his busy schedule to calibrate our probe tube microphones. Also thank you to Prof. John Rosowski for sharing his expertise on high-frequency acoustics.

We owe a big thank you to Prof. Lisa Olson and her group at Columbia university, especially Wei Dong and Ombeline de la Rochefoucauld for demonstrating their surgical and measurement techniques to help us get started on our experiments. Also thanks to Prof. Nigel Cooper for sharing his expertise on live animal surgery and laser targets. Thank you to Prof. Charlie Liberman for his advice and assistance. The following people were very helpful general academic advisors in my first two years at MIT: Prof. Antonio Torralba, Prof. Isaac Chuang, and Prof. Leslie Kolodjiejski.

I would like to thank the National Science and Engineering Research Council of Canada (NSERC) for their financial support during the time of this study. Thank you to my advisors in Canada who were instrumental in allowing me to receive the NSERC funding: Prof. John Pezacki, Prof. Gerardo Diaz-Quijada, and Prof. Albert Leung.

For their help with ordering parts and supplies, thank you to Janice Balzer and John Sweeney. Also thank you to Lourenco Pires for his technical advice on circuit design.

I am very grateful to the following people for sharing their expertise on animal housing, handling, and surgery: Dr. Alison Hayward, Catrina Wong, and Suzette Alvarado.

I'd like to thank all of my friends at MIT and in Vancouver who were supportive throughout my time doing this research: Albert Chang, Ann Hickox, Carlijn Mulder,

Chrysa Samara, Daniel Prashanth, Jo Hayden-Sommerton, Joy Johnson, Katarina Blagovic, Leon Li, Mimi Wu, Olha Lui, Oshani Seneviratne, Pavitra Krishnaswamy, Salil Desai, Sarah Paydavosi, Sheila Nabanja, Tissa Mirfakhrai, and Wayne Chen.

Finally, I'd like to thank my family for helping me get to this point and for their continued love and support. Thank you to my parents, Hengameh Hamavand and Bijan Farrahi. Thanks to my sister, Katayoun, and her husband, Farzad (also for his advice on surgery). And last but certainly not least, thank you to my husband, Arya Farahmand, for his continuous love, support, and sense of humor.

Contents

List of Figures

THIS PAGE INTENTIONALLY LEFT BLANK

Chapter 1

Introduction

A major goal in the field of cochlear micromechanics is to gain a deeper understanding of the basic processes underlying motion of the cochlea, an amazing biological structure. This understanding not only has the potential to help understand the processes underlying hearing disorders, but it can also lead to the design of more efficient, biomimetic mechano-electric transducers. Since the properties of the cochlea change drastically on death, it is important to be able to take measurements of live cochleae. Therefore, the goal of this study was to measure micromechanical motion in an in vivo mammalian cochlea. The chosen measurement technique was Laser Doppler Velocimetry (LDV), and the chosen mammal was the Mongolian gerbil. Ultimately, we wish to measure the micromechanical properties of cochleae in mouse models of genetic hearing disorders. However, the mouse's small size makes it a challenge. Therefore, as a first step, the development of motion measurements on gerbil cochleae gave us valuable insights on the various methods required including animal surgery, high-frequency sound delivery and calibration, and LDV measurement techniques. In addition, the gerbil cochlea allows us to answer some outstanding questions about the intricate micromechanical motions of the cochlea and how they may affect mammalian hearing.

To reduce the number of variables in our experimental development, we chose a commercial LDV, similar to those which have been used for similar measurements in prior studies. In previous work, glass beads of 10 to 30 μm diameter were placed on the

basilar membrane (BM) to increase the reflectivity of the tissue to the incident laser beam. The microbeads were placed through the round window (RW) or through a small hole in the cochlea. We chose to introduce beads through the RW as an attempt to cause the least damage to the animal's hearing.

This chapter will describe the known properties of the mammalian hearing organ and the principle of operation of laser Doppler velocimetry. Chapter two describes the methods used to perform laser velocimetry, measure the sound pressure level in the animal's ear, gain access to the gerbil cochlea, and perform compound action potential (CAP) measurements to assess the health of the gerbil's hearing. Chapter three describes the LDV and CAP results obtained. Chapter four describes the implications of the results. Chapter five presents a conclusion.

1.1 The Mammalian Cochlea

The mammalian cochlea is a micromechanical transducer with five orders of magnitude of sensitivity over a frequency range of 20Hz to 20kHz, with the lowest detectable sounds producing vibrations on the order of the diameter of an atom. These amazing properties have been the focus of years of research, yet there are still many mysteries of how the ear operates. In this section, some of the known properties of the cochlea will be summarized.

When sound travels to the ear drum, or tympanic membrane, it causes vibrations which are transmitted through the air-filled middle ear to the fluid-filled cochlea via the three middle ear bones (the malleus, incus, and stapes). These bones serve to match the impedance between the external air and the fluid in the cochlea, thus maximizing sound transmission, and are one of the key features of the mammalian cochlea. The cochlea, which comprises the part of the inner ear responsible for hearing, is formed from three fluid-filled chambers which spiral from the base near the stapes to the apex. The Mongolian gerbil cochlea is made up of three turns and has a total length of 12 mm [9].

When the stapes moves, it pushes the oval window, causing the cochlear partition

to move and the round window membrane (RWM) to move out. Since the fluid inside the cochlea is incompressible, the RWM serves to relieve the pressure caused by the motion of the stapes.

The basilar membrane (BM) is tuned to vibrate maximally at different frequencies, with the highest frequency sounds causing the greatest vibrations at the base of the cochlea close to the stapes, and lower frequency sounds causing maximal vibrations toward the apex of the cochlea. Furthermore, the relationship between frequency and location in the cochlea is approximately logarithmic. For example, in the human cochlea, the maximal frequency of response (or best frequency) approximately doubles for every 5 mm closer to the stapes. In the Mongolian gerbil, this number is 1.5 mm.

The critical cells in the cochlear partition as shown in figure 1-1 are the hair cells which come in two types: inner and outer hair cells. The inner hair cells are responsible for transducing the motion of the cochlear partition into electrical signals sent to the brain; whereas, the outer hair cells are believed to play a role in amplifying the motion of the cochlear partition.

1.2 Effect of Death on Cochlear Micromechanics

The first BM motion recordings in mammals were performed on human cadavers by Georg von Békésy [18]. Studies have shown significant changes in BM responses in dead vs. live animals. The BM in a dead animal is much less frequency selective, having a much smaller Q value as shown in figure 1-2. In addition, the live cochlea exhibits compressive non-linearity whereby doubling the sound pressure will cause an increase in BM motion of less than a factor of two. Compressive non-linearity also disappears after death. These changes are believed to be due to the loss of the active amplification provided by the outer hair cells as well as the loss of potential differences across the hair cells in the organ of Corti.

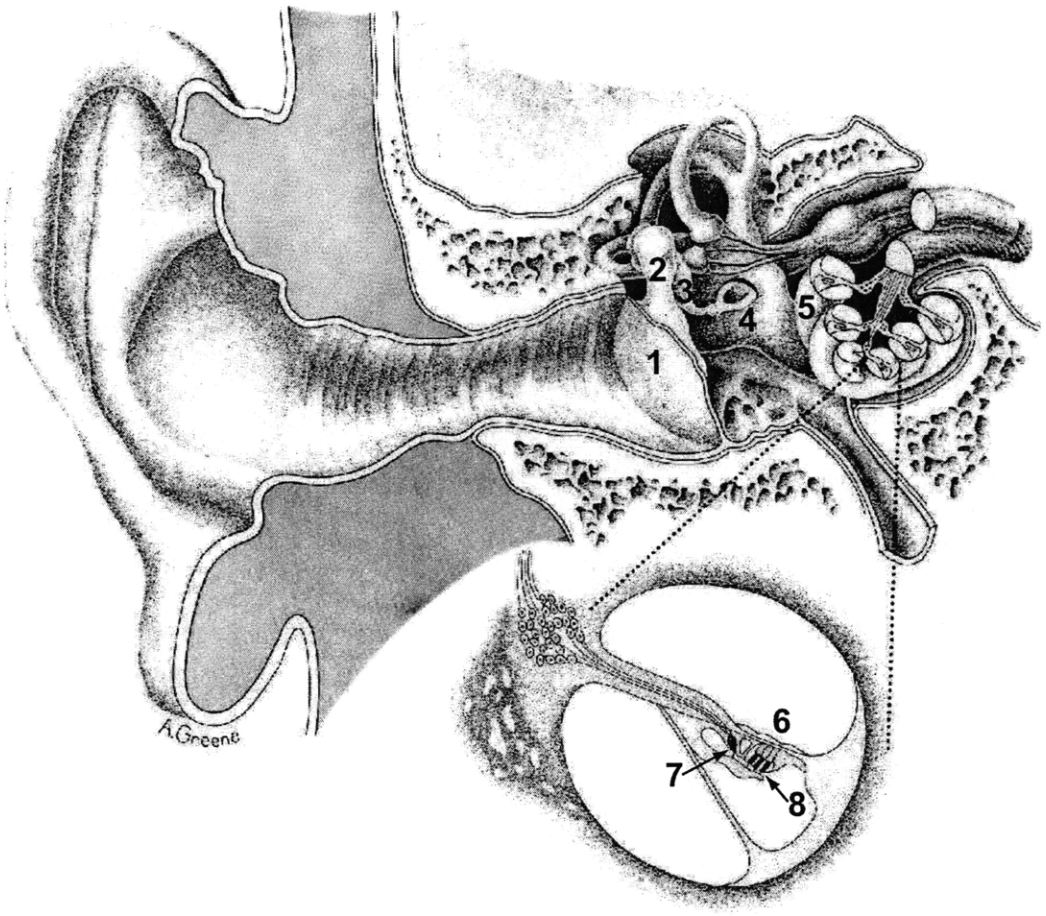

Figure 1-1: Anatomy of the human ear showing the ear canal through which sound enters, the middle ear bones, and a cross-section of the spiraling inner ear or cochlea. Numbered structures: 1) Tympanic membrane (ear drum) 2) Malleus 3) Incus 4) Stapes 5) Cochlea (base near top of image, apex further down) 6) Basilar membrane 7) Inner Hair Cell 8) Outer hair cells

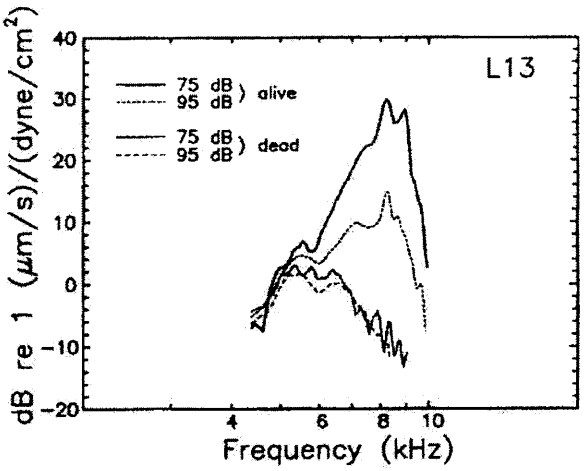

Figure 1-2: Frequency response of BM velocity for dead vs. alive animals (taken from [15])

1.3 Laser Doppler Velocimetry

Early in vivo recordings of BM motion were done using the Mössbauer technique [7]. This technique involves the placement of a radioactive source on the tissue being studied and measurement of the resulting radiation. The Mössbauer technique led to the discovery of the compressive nonlinearity of the BM [14]. Laser velocimetry has overtaken the Mössbauer technique for studies of cochlear mechanics because the Mössbauer technique is highly nonlinear outside of a small range of motions, and its sensitivity is lower than laser velocimetry.

Laser velocimetry involves two laser beams (one reference beam and one sample beam) with frequency difference Δf. The two beams recombine and produce a beat signal with frequency Δf measured by a photodetector as shown in 1-3. The frequency of the beat signal is modulated by the velocity of the target. The intensity of light at the photodetector is given by

$$I(t) = I_R I_S R + 2K\sqrt{I_R I_S R}\cos(2\pi(f_D)t + \Phi),$$

where I_R is the intensity of light in the reference beam and I_S is the intensity of light in the sample beam. R and K are mixing coefficients. This leads to the Doppler

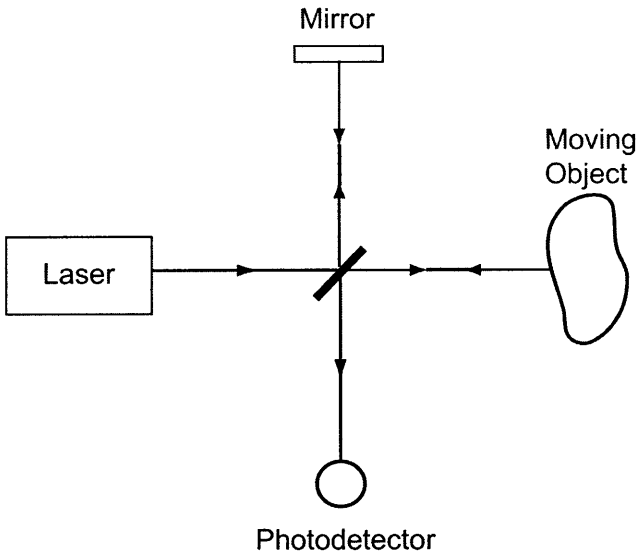

Figure 1-3: Diagram of a simple homodyne velocimeter. The laser beam is split into a reference path which hits the mirror and a sample path which hits the object. The two then recombine at a photodetector, producing a signal which can be analyzed to obtain the velocity of the target.

frequency, f_D.

$$f_D = 2v/\lambda,$$

where v is the velocity of the target, and λ is the wavelength of the laser light.

In heterodyne velocimetry, an acousto-optic modulator, or Bragg cell, is used to provide a difference in frequency between the reference beam and the sample beam of the interferometer as shown in figure 1-4. The beat signal measured at the photodetector will be given by

$$I(t) = I_R I_S R + 2K\sqrt{I_R I_S R}\cos(2\pi(2f_B - f_D)t + \Phi),$$

where f_B is the frequency of the Bragg cell. Heterodyning allows forward and backwards movements to be differentiated. In homodyne velocimetry, forward and backwards movements appear identical. In this study, we used a heterodyne velocimeter as outlined in the next chapter.

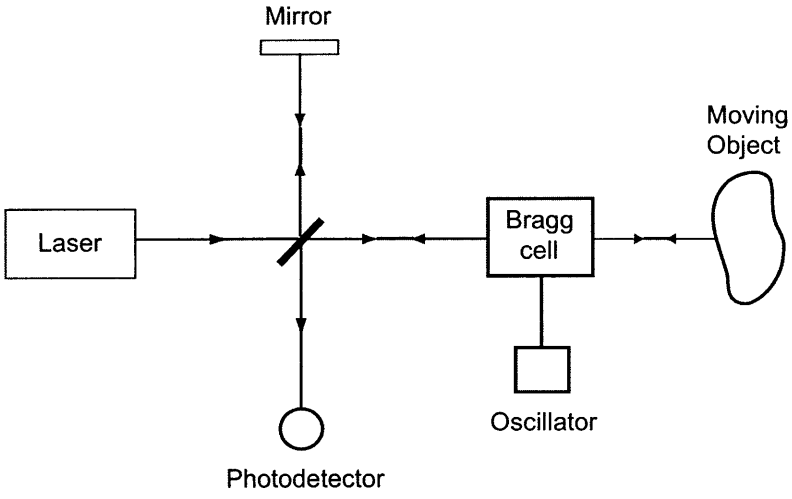

Figure 1-4: Diagram of a heterodyne velocimeter. The reference beam does not pass through the Bragg cell while the sample beam passes through it twice, leading to a frequency difference between the two beams of $2f_B$.

THIS PAGE INTENTIONALLY LEFT BLANK

Chapter 2

Methods

In this chapter, the methods used for surgery, sound delivery, and laser Doppler velocimetry (LDV) measurements are described.

2.1 Animal Preparation

Mongolian gerbils (n=72; 1-6 months old) were used in this study. Many of these animals served to develop and enhance the methods described below. The preparation and use of the experimental animals were approved by the Committee on Animal Care at MIT. Gerbils were anesthetized with an intraperitoneal injection of urethane (Sigma-Aldrich, 1.2g/kg). Anesthesia boosts at half the original dose were administered as deemed necessary from the animal's response to a toe pinch every 30 minutes. Subcutaneous injections of Ringer's solution were delivered every hour to keep gerbils hydrated (Hospira Inc., 10mL/kg). Once sedation was achieved, a tracheotomy was performed to reduce motion of the head during breathing. The skin and hair were removed from the posterior surface of the head to allow attachment of an aluminum head holder. The head holder was attached to a micromanipulator allowing fine positioning of the head. The pinna and tissue surrounding the right auditory bulla were removed and a hole was made in the bone on the ventral side of the ear canal (EC) to allow placement of the probe tube near the umbo. The sound delivery system was secured to the EC using Krazy glue (Elmer's Products Inc.) as

shown in figure 2-1. A hole was made in the bulla by shaving the bone carefully with a number 11 scalpel blade to provide visual access to the round window (RW). A small hole was made in the RW membrane (RWM) using a curved stainless steel pin, and beads were allowed to settle on the BM below. When possible, a coverslip was placed over the RW to reduce any fluid motion and control the fluid meniscus. Body temperature was monitored rectally and maintained at 38 $\pm$3°C using a heating pad. Heart rate was also monitored to assess the depth of anesthesia. Upon completion of measurements in live preparations, the animals were euthanized with an overdose of urethane and cervical dislocation. Post mortem measurements were done after the animal had been dead for anywhere between one to eight hours. The bullae of the dead animals were filled with artificial perilymph to ensure that the tissue did not dry out. The fluid was removed before post-mortem measurements were begun.

2.2 Sound Delivery

The sound system consisted of a System 3 from Tucker Davis Technologies (TDT), including an ED1 speaker driver and an EC1 electrostatic speaker. Pure tone signals for BM motion measurements were delivered to the ED1 using a waveform generator (Hewlett Packard 33120A) while tone pips for CAP recordings were generated using a digital to analog converter card on a computer (Interface Corporation PCI-3525). We used a custom-made passive attenuator to lower the amplitude of signals from the waveform generator by 20 or 40dB as necessary. We also used an eleven-pole elliptical function lowpass filter with a cutoff frequency of 100kHz (TTE, Inc.). The entire sound delivery and data acquisition system are shown in figure 2-2.

Sound was coupled to the EC and sound pressure at the EC was measured as shown in figure 2-1. Sound was coupled from the EC1 to the ear canal using 10 cm of flexible tubing (Tygon 2.4 mm inner diameter), with a short brass section which fit telescopically into the brass tube glued to the EC (3.2 mm inner diameter). The probe tube used to measure sound pressure level in the EC fit into a notch in the brass tube cemented in the EC and was brought close to the umbo using a micromanipulator.

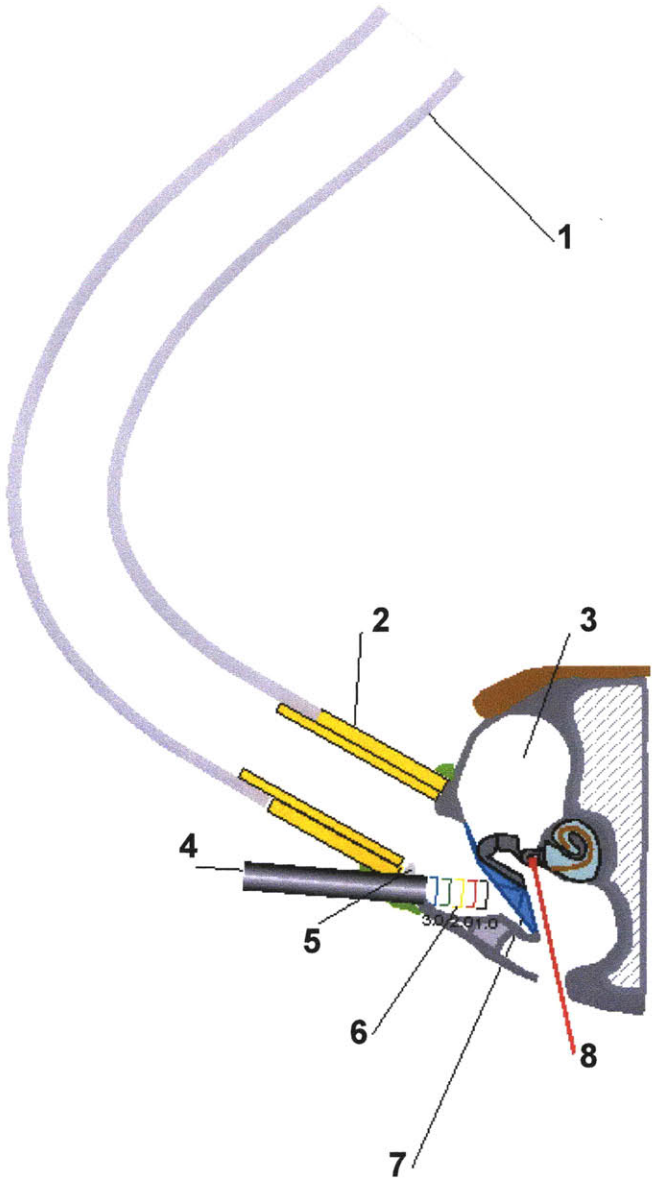

Figure 2-1: Diagram of gerbil EC, sound delivery tubes, and probe tube placement. 1) Plastic tube 2.5 mm ID. 10 cm long. 2) Sound coupler sealed around bony ear canal opening 3) Middle-ear spaces 4) Moving microphone probe tube 5) Remove part of bony ear canal wall 6) Locations of probe tube tip 7) Tympanic membrane 8) Laser focused on target on posterior stapes crus through hole in bulla wall. (by M. Ravicz, included with permission)

Figure 2-2: Picture of equipment used in experimentation 1a) TDT ED1 speaker driver 1b) TDT EC1 electrostatic speaker 2) HP33120A function generator 3) Personal computer used to control signal generation and data acquisition 4) Amplifier for probe tube microphone signals 5) Programmable attenuator 6) Polytec interferometer controller 7) Sound-proof chamber (not visible. In background of picture)

2.2.1 Sound Level Calibration

The probe tube system consisted of a MEMS microphone (Knowles Acoustics, SPM0204UD5) coupled to a 10 mm probe tube constructed of hypodermic tubing (Small Parts, 18 gauge thin-wall, 0.97 mm inner diameter). The microphone and probe tube were coupled with a plastic cone intended to reduce any acoustical reflections due to sharp discontinuities. The acoustic effect of the probe tube and plastic cone setup was corrected using the method of M. Ravicz as described in [12].

The probe tube design allowed reliable measurement of sound pressures in the EC because of the small diameter of the probe tube tip, meaning that the size of the cavity being measured did not have a significant effect on the signals obtained. Nevertheless, the probe tube correction was performed in a chamber designed to have the same volume as the gerbil EC. The probe tube was placed in this chamber within 0.3 mm of a reference microphone. As sound was played from 100Hz to 100kHz, the responses of both microphones were measured. The difference in magnitude and phase between our probe tube microphone and the reference microphone was taken as the correction applied to the voltages read by the microphone in order to obtain sound pressures at the tip of the probe tube in the gerbil EC as shown in figure 2-3. The probe tube sensitivity was measured before each experiment to ensure that its acoustic properties had not changed. The voltage signal obtained from the probe tube microphone during each measurement was corrected by the magnitude and phase values at each frequency shown in figure 2-3. After the correction is applied, the voltage corresponding to sound at the probe tube tip is known. Obtaining sound pressure from this voltage is a linear conversion.

Since the receptive field of the probe tube setup extends to roughly 0.6× the probe tube radius [1], the probe tube was inserted to at least 0.3-0.4 mm inside the EC for frequencies up to 30 kHz and roughly 0.3-0.4 mm from the tympanic membrane (TM) for frequencies above 30 kHz [12].

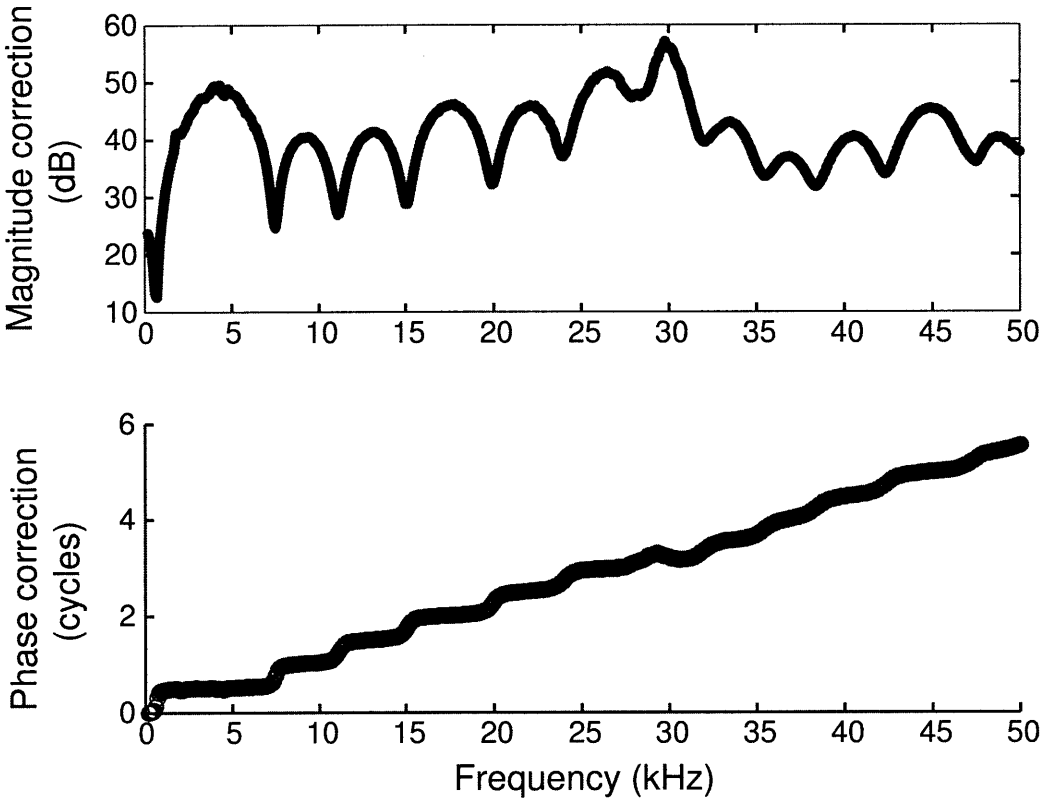

Figure 2-3: Probe tube calibration. The magnitude correction gives the ratio of the reference microphone and the probe tube microphone in dB. The phase correction gives the difference between the phase of the reference microphone and the probe tube microphone in cycles.

2.3 Laser Doppler Velocimetry

In this study, we used the Polytec OFV 3001/511 heterodyne interferometer because it was the most easily accessible and has comparable noise and bandwidth parameters to other systems used in basilar membrane motion studies. The interferometer was coupled to an upright microscope (Carl Zeiss Inc.) so that the beam passed through a 10X objective lens, making the total magnification 100X. The laser beam reflected off of the target tissue and passed through the same objective lens to be collected and processed by the interferometer. The interferometer and microscope were on an air table inside a sound-proof enclosure (Integrated Dynamics Engineering Inc.). Sound delivery and response recording were both performed using the same personal computer shown in figure 2-2.

In order to reduce noise in the laser Doppler signal, a digital FIR filter centered at the stimulus frequency was used to filter the signal detected by the computer's analog to digital converter. Responses were only recorded if the raw laser Doppler signal power spectrum had a significant peak above the noise floor. At each frequency, the response was determined as the average peak magnitude over 30ms of sampled data with a rate of 1 megasamples/second. The magnitude and phase at each frequency were determined using a least-squares method of fitting a sinusoid to the raw sampled data. All of the BM measurements were taken with a velocity factor of 5 mm/s/V on the interferometer. At this setting, the corner frequency of measurement was 100,000 Hz.

To validate our measurement system, we used a Doppler optical coherence microscopy (DOCM) system and measured the same piezo-electric crystal under identical stimulus conditions. The results of this test are shown in figure 2-4. We see that there is a constant phase delay in the LDV measurement relative to the DOCM measurement. This is due to a known phase delay parameter in the Polytec system and is corrected in all subsequent LDV measurements presented.

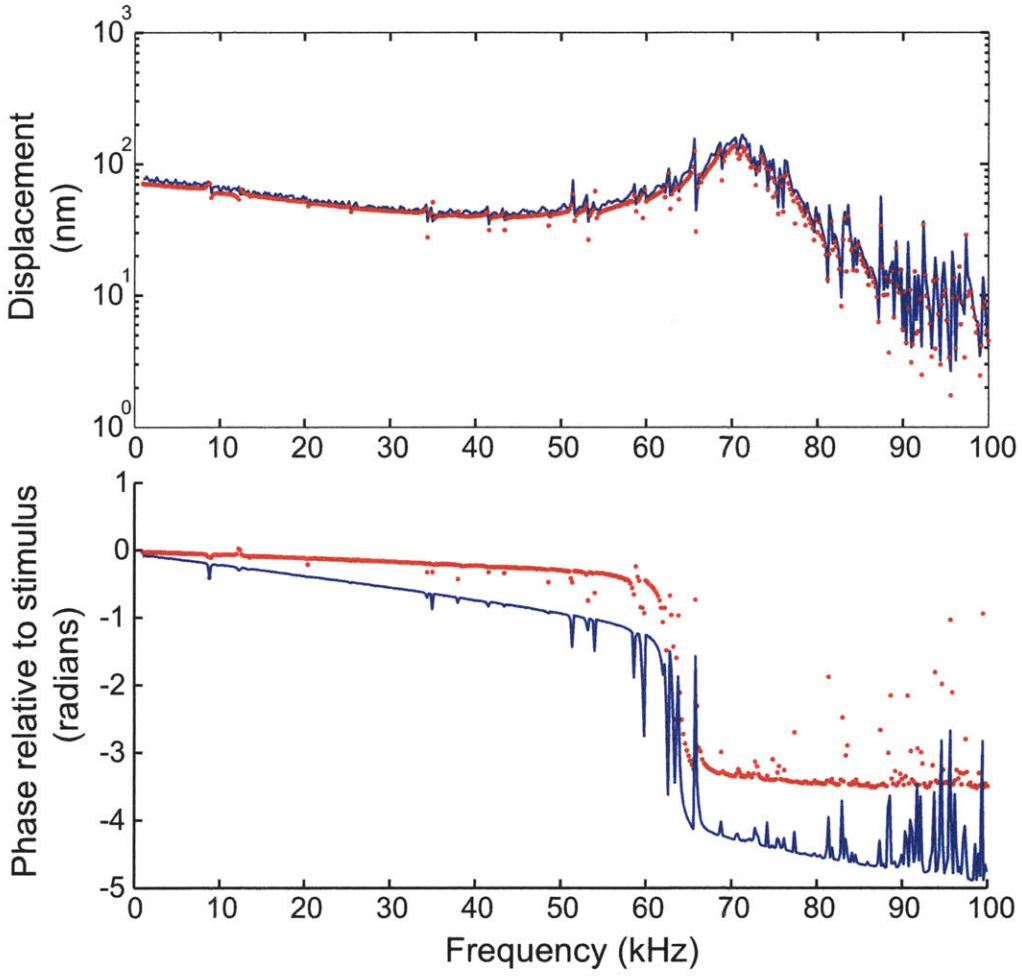

Figure 2-4: Comparison of LDV measurements with a different interferometric based system (Doppler optical coherence microscopy or DOCM). Comparison of piezo-electric crystal displacement in LDV (solid) and DOCM (dots). This particular piezo-electric crystal showed a resonant peak at roughly 70kHz with a corresponding half-cycle phase lag. Magnitude shows peak-to-peak displacement in both systems, and phase is measured relative to the stimulus.

2.3.1 Bead Properties

In this study, 10 μm polystyrene beads (Polysciences Inc.) were used, and imaging was done in the basal region of the gerbil cochlea. The beads were sputter coated with 50 nm of gold to increase their reflectivity to the laser beam when the beads were submerged in the perilymph of the cochlea. A 5 nm layer of titanium was initially sputtered onto the beads as an adhesive aid. The density of the beads was roughly 1050 kg/m^3, or only slightly greater than the density of water.

2.3.2 Measurement of Laser Spot Size

The size of the laser spot was measured using a photodector (New Focus Inc.), razor blade, and micromanipulator stage. The photodetector was placed under the microscope objective such that the laser beam shone on the photodector surface. The razor blade was mounted to the micromanipulator stage such that it could be moved over the photodetector to gradually block the path of the laser beam on the photodetector. The razor blade was moved in 1μm steps, and the DC voltage on the photodetector was recorded with each step. A sigmoidal curve of power vs. distance was thus obtained. An error function was fit to the data as shown in figure 2-5. The laser spot size was estimated as the full-width half maximum of the error function fit, or roughly $2.35 \times \sigma = 2.35 \times 0.662 = 1.56\mu$m. The accuracy of this method is limited by the distance between the photodetector and razor blade edge due to diffraction effects which will cause the beam size to be overestimated. For this reason, the distance between the razor and photodetector was minimized as much as possible and was roughly 0.5mm.

2.3.3 Control Measurements

To ensure that our measurements were responses to the sound delivered to the EC, each experiment included an identical measurement of a bead with the sound source turned off. In addition, when possible, beads that had landed on the spiral lamina next to the BM were measured to determine the motion due to the fluid meniscus.

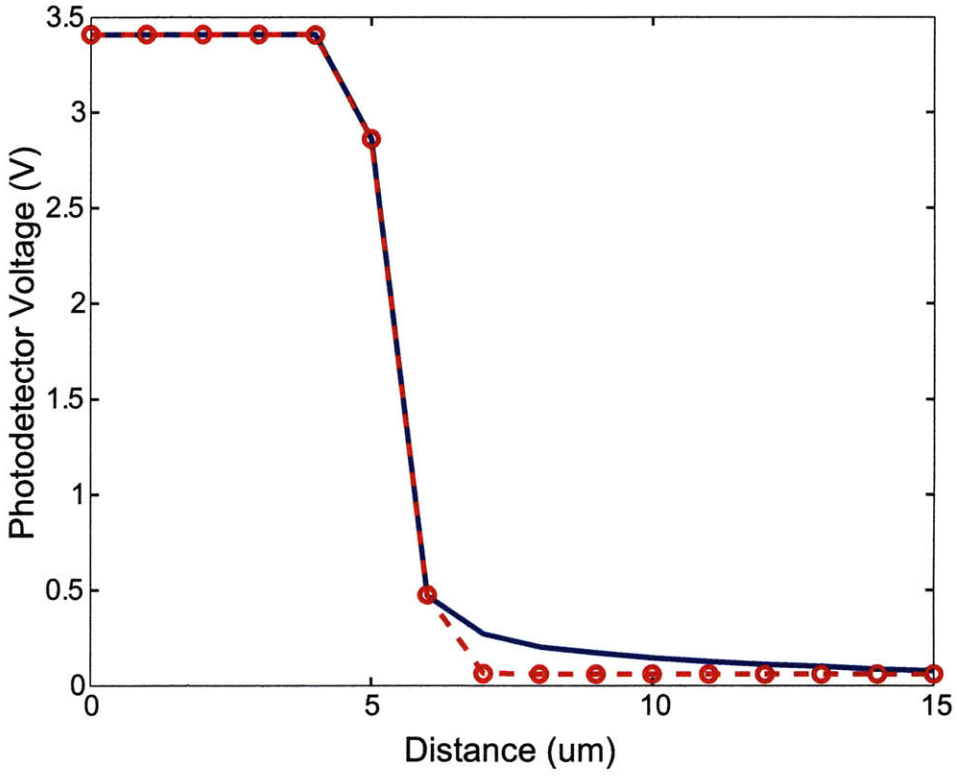

Figure 2-5: Photodetector data used to determine laser spot size (solid) and error function fit used to estimate standard deviation of data (-o-)

When a coverslip could be placed on the RW while maintaining visual access to the BM and beads, beads on the coverslip were also measured. Measurements were always repeated to determine the stability of the preparation and as another measure of noise.

2.4 Compound Action Potential Measurement

After adequate bead placement was obtained, we measured a baseline compound action potential (CAP) to assess the gerbil's hearing sensitivity over frequency. To obtain a CAP spectrum, we used three electrodes: one in the RW, another near the trachea, and the third near the tail. The RW electrode was a silver wire. The differential signal between the RW and chest was amplified 10,000×. Tone pip stimuli were delivered at a maximum rate of 10 per second. Tone pips were 5 ms in duration with sinusoidal growth and decay shapes. Alternate tone pips were delivered with alternating polarity to eliminate the cochlear microphonic due to the AC current through the hair cells in the organ of Corti. At least 50 tone pips were delivered and the responses averaged to reduce the effect of electrical noise. CAP thresholds were determined to within ±5 dB SPL in the range 15 - 100 dB SPL. A CAP spectrum was re-measured at the end of the experiment if the animal's hearing was believed to have changed for any reason.

THIS PAGE INTENTIONALLY LEFT BLANK

Chapter 3

Results

In this chapter, the Laser Doppler Velocimetry (LDV) and Compound Action Potential (CAP) results for three gerbils will be presented.

3.1 Laser Doppler Velocimetry

3.1.1 Control Experiments

To test our experimental measurements, we performed the following experiments: 1) measured the gerbil stapes and compared our results to those obtained by other groups using a similar experimental setup; 2) measured beads on the basilar membrane (BM) with sound on and off; 3) measured a bead on the BM with and without a coverslip over the RWM to determine how much of our measurements are affected by fluid artifacts; and 4) measured beads on the BM with the ear canal (EC) sealed and unsealed. The results of each test are summarized below.

1) We measured the frequency response of the gerbil stapes and compared the results to those obtained by Ravicz, Cooper and Rosowski [11]. The stapes response is less sensitive to variations in each animal's hearing and is thus an easier reference for comparison with other research groups. The approximate angle of measurement used is shown in figure 2-1. The magnitude and phase responses that we obtained by measuring the response of a bead on the posterior crus of the gerbil stapes are

shown in figure 3-1 along with a measurement obtained by Ravicz, Cooper, and Rosowski [11]. The magnitudes of the two responses differ by less than 20 dB over all frequencies while the phases differ by less than one-half cycle. Furthermore, both responses decrease with roughly the same rate with frequency and show similar group delays.

2) In each animal, measurements were repeated with the sound stimulus turned off but all other elements of the system turned on. This provides an estimate of noise in the LDV measurements and suggests that our measurements are in response to sound and not an artifact of the system. As shown in figure 3-2, the velocity response obtained with the sound turned off was 10 to 1000 times smaller than with the sound on.

3) We measured a bead on the BM with and without coverslips over the RW to determine the effect of fluid motions on our measurements. Figure 3-3 shows the same bead measured with no coverslip vs. two coverslips on the RW. Two coverslips were used to provide added weight to suppress any fluid motions in the RW. The two responses differ by less than 12dB in magnitude and less than one quarter cycle in phase.

4) We measured a bead on the BM with and without sealing the space around the EC to determine whether or not sealing the EC was necessary. The seal was made with Vaseline. Many of the measurements presented here were done without sealing the space around the probe tube in the EC (see figure 2-1). As shown in figure 3-4, the difference in magnitude between the sealed and unsealed response was less than 6dB while the difference in phase was less than one quarter cycle.

3.1.2 BM Frequency Responses

Figure 3-5 shows the response of a bead on the BM when the animal was alive and after it had died. The bead was roughly in the middle of the BM as shown in panel A. As we can see, the response of the same bead dropped by roughly 20dB after the animal died. The best frequency (BF) also dropped by half an octave (from roughly 34 kHz to 24 kHz) after the animal died. In addition, the phase of the dead response

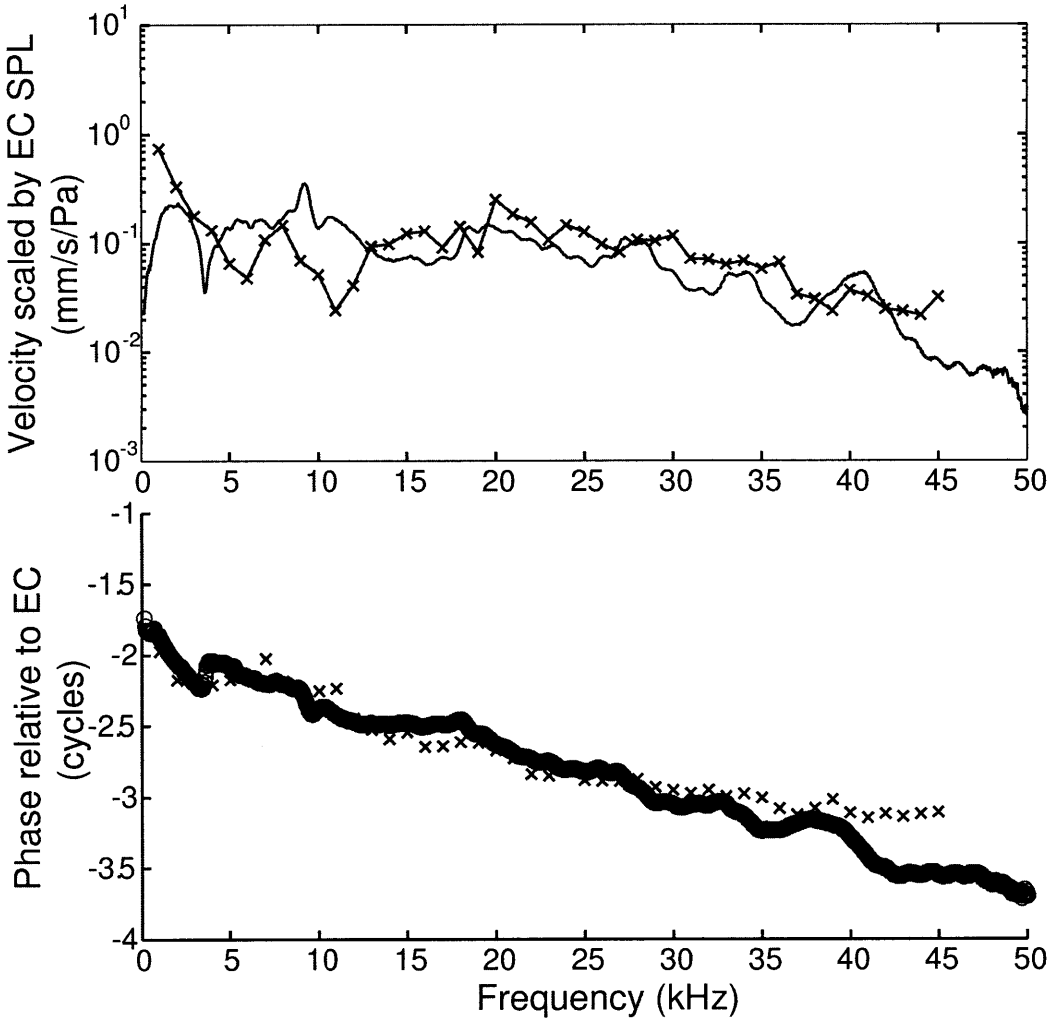

Figure 3-1: Gerbil stapes frequency response. Comparison of our measurement system (x) vs. that shown in figure 4b) of Ravicz, Cooper, and Rosowski [11] (solid). Magnitude is given as velocity in mm/s normalized by the sound pressure in Pascals as measured in the ear canal with the probe tube microphone. The phase is given as cycles relative to the phase at the EC. Our data were measured with 1kHz spacing while the data of Ravicz, Cooper, and Rosowski were measured with 100Hz spacing.

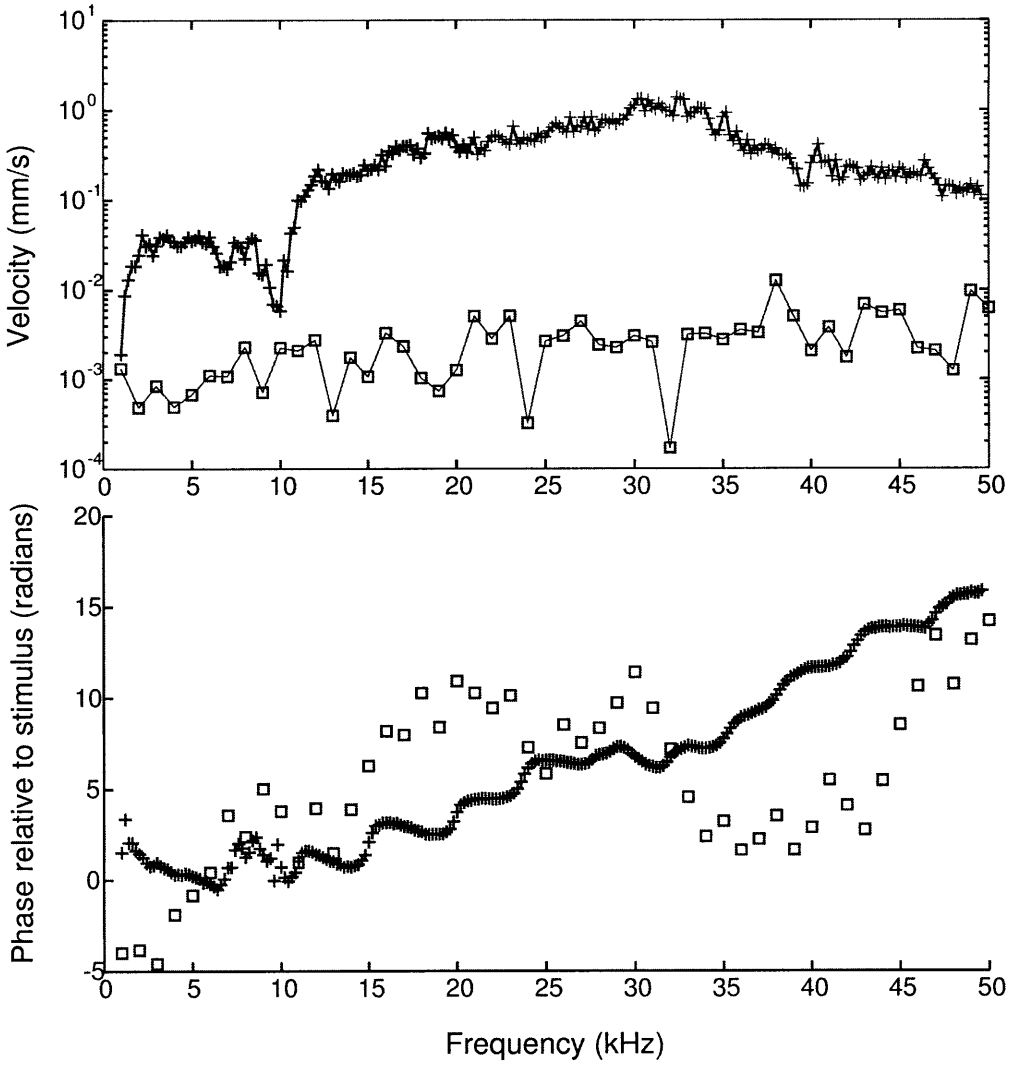

Figure 3-2: Response of a bead on the gerbil BM with (*) and without (square) sound stimulus. Both measurements were done on a live animal. Magnitude is given as velocity and phase is given as radians. Neither response is corrected for the sound pressure in the EC.

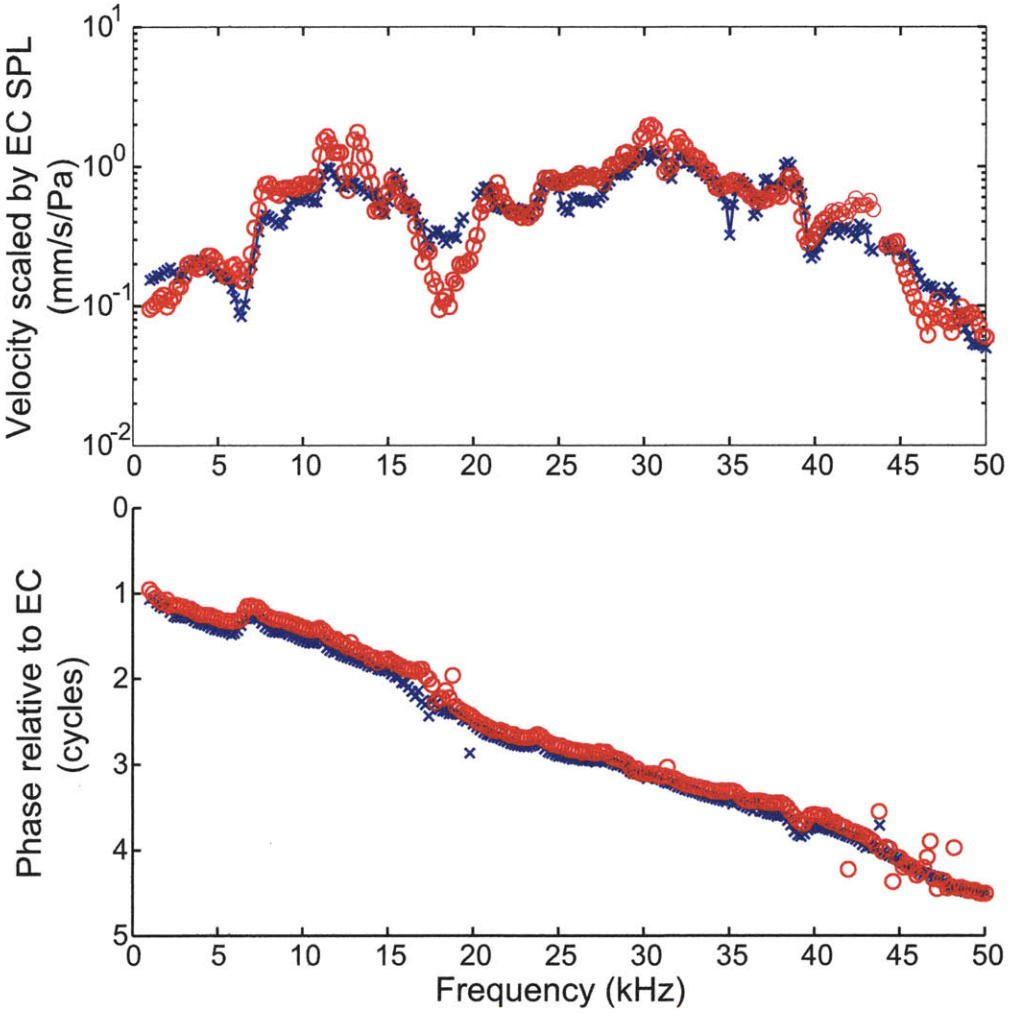

Figure 3-3: In vitro gerbil BM response with (solid) and without (x) two coverslips on RW. Magnitude data was smoothed using a three-point average method. The signal quality on the interferometer in the case with two coverslips was not as good as the case without any coverslips, so this may have lead to differences in magnitude.

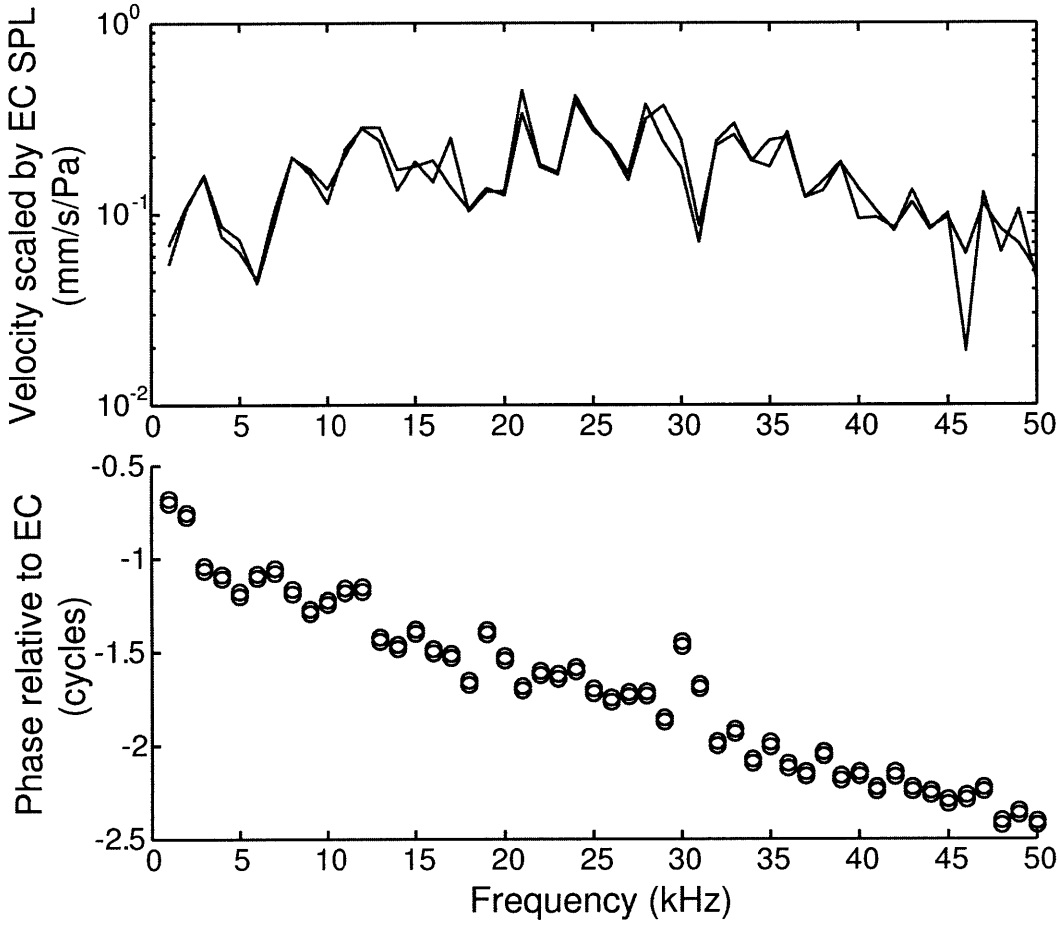

Figure 3-4: In vitro gerbil BM response with and without a sealed EC. The signal quality on the interferometer in the two cases was not identical, so any difference in magnitude between the two responses could be attributed to the difference in signal quality.

led the live phase response below the BF and lagged the phase response of the live response past the BF. Regarding the sensitivity of the live response, we see that the peak is 34dB above the lowest response at 1kHz. In addition, the total phase accumulation is 2 cycles with a slight increase in group delay above the BF. The CAP threshold curve for this animal when it was alive and all of the beads had been placed on the BM is shown in figure 3-9.

3.1.3 Radial Differences in Motion along BM

In the live gerbil with the most sensitive hearing, we measured two beads along the BM and one on the bone. Figure 3-6 shows the relative locations of the three beads and their frequency responses when the animal was alive. We can see that the bead closer to the center of the BM has a larger response than the one on the edge of the BM. If we measure the Q_{10dB} values as shown below for the smaller response, we get $Q_{10dB} = 3.09$ for the larger response and $Q_{10dB} = 2.19$ for the smaller response.

$$Q_{10dB} = \frac{CenterFrequency}{3dBBandwidth} = \frac{34{,}000}{38{,}500-23{,}000} = 2.19$$

The larger response is the same bead shown in figure 3-5. The beads were not equidistant from the stapes, and the total distance between them was measured to be 80μm. The bead on the bone away from the BM shows no significant peaks in the magnitude response. It is also worth noting that the responses of both beads on the BM in this figure showed similar changes after the animal died. That is, the peak responses dropped and shifted by roughly one half octave (not shown).

In two other animals, the responses of two beads at different radial positions on the BM were measured post-mortem. One of these cases is shown in figure 3-7. We can see that the bead closer to the center of the BM has a larger response but that the peaks have roughly the same widths. Indeed, if we take the peak magnitude response of both responses in figure 3-7 and find the points on either side of the peak where the magnitude has dropped by 10dB, we see that the 10dB bandwidths of the two responses differ by less than 5%. In this case, the larger response had $Q_{10dB} = 2.1$ and the smaller response had $Q_{10dB} = 2.2$.

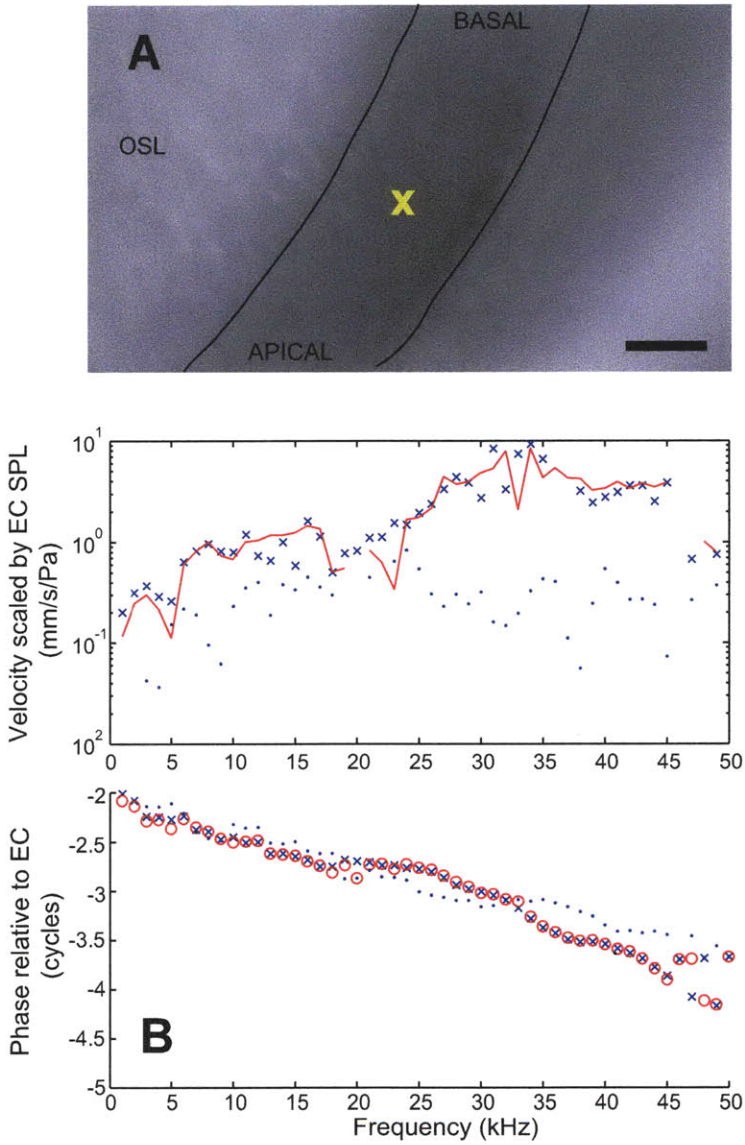

Figure 3-5: In vivo vs. In vitro BM responses. Panel A shows an image of the gerbil BM with the approximate location of the bead whose frequency responses are shown in panel B with the animal alive (solid and x) vs. dead (dots). The picture of the BM was taken with an upright microscope at 50X magnification. The BM is outlined with apical and basal directions indicated. OSL = osseous spiral lamina. The two live measurements were taken roughly one hour apart to assess the stability of the live preparation. The magnitude response is given as the velocity in mm/s normalized by the sound pressure in Pascals as measured in the EC with the probe tube microphone. The sound pressure delivered to the ear canal was roughly 80 dB SPL. The phase is given as cycles relative to the phase at the EC. (Scale bar = 100μm)

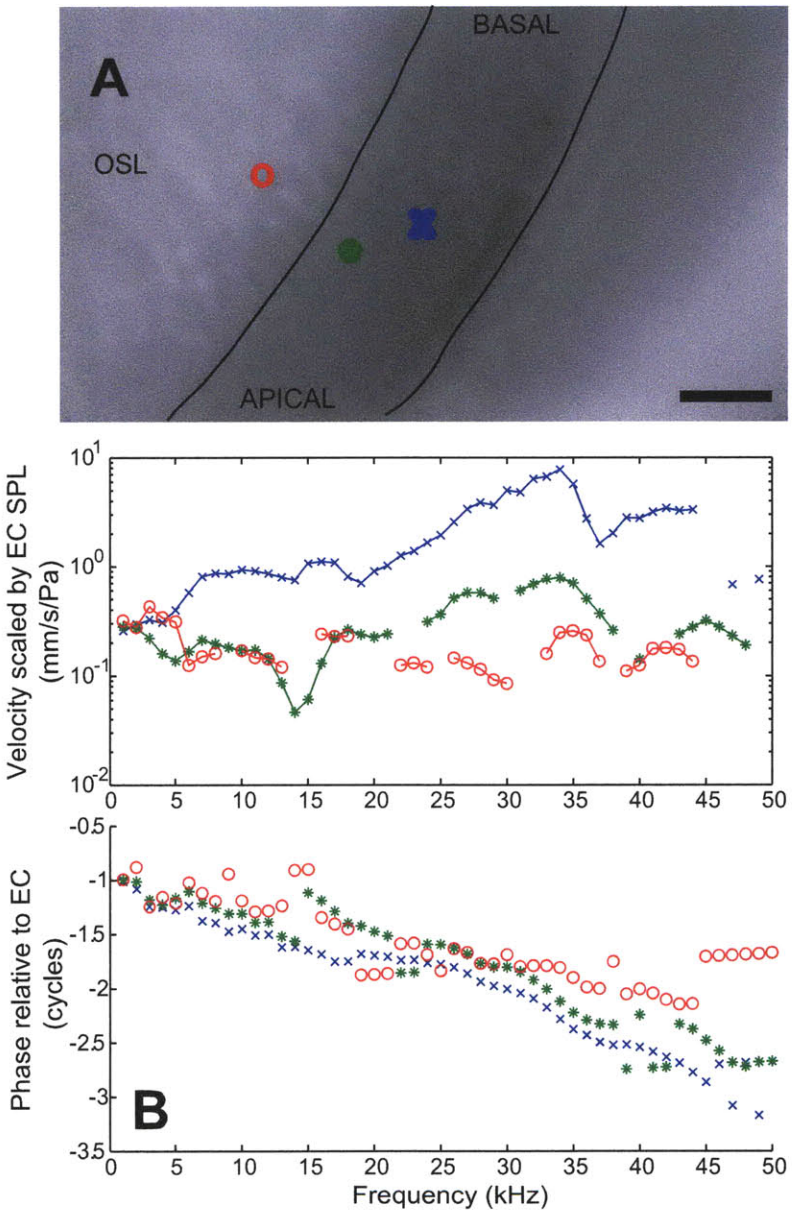

Figure 3-6: In vivo responses along the radius of the BM. Panel A shows an image of the gerbil BM with the approximate locations of the beads whose frequency responses are shown in panel B (Scale bar = 100μm). The picture of the BM was taken with an upright microscope at 50X magnification. The BM is outlined with apical and basal directions indicated. OSL = osseous spiral lamina. Symbols representing responses in Panel B correspond to the same symbols in Panel A. The magnitude response is given as the velocity in mm/s normalized by the sound pressure in Pascals as measured in the ear canal (EC) with the probe tube microphone. The magnitude responses were smoothed using a three-point mean. The sound pressure delivered to the ear canal was roughly 100 dB SPL. The phase is given as cycles relative to the phase at the EC.

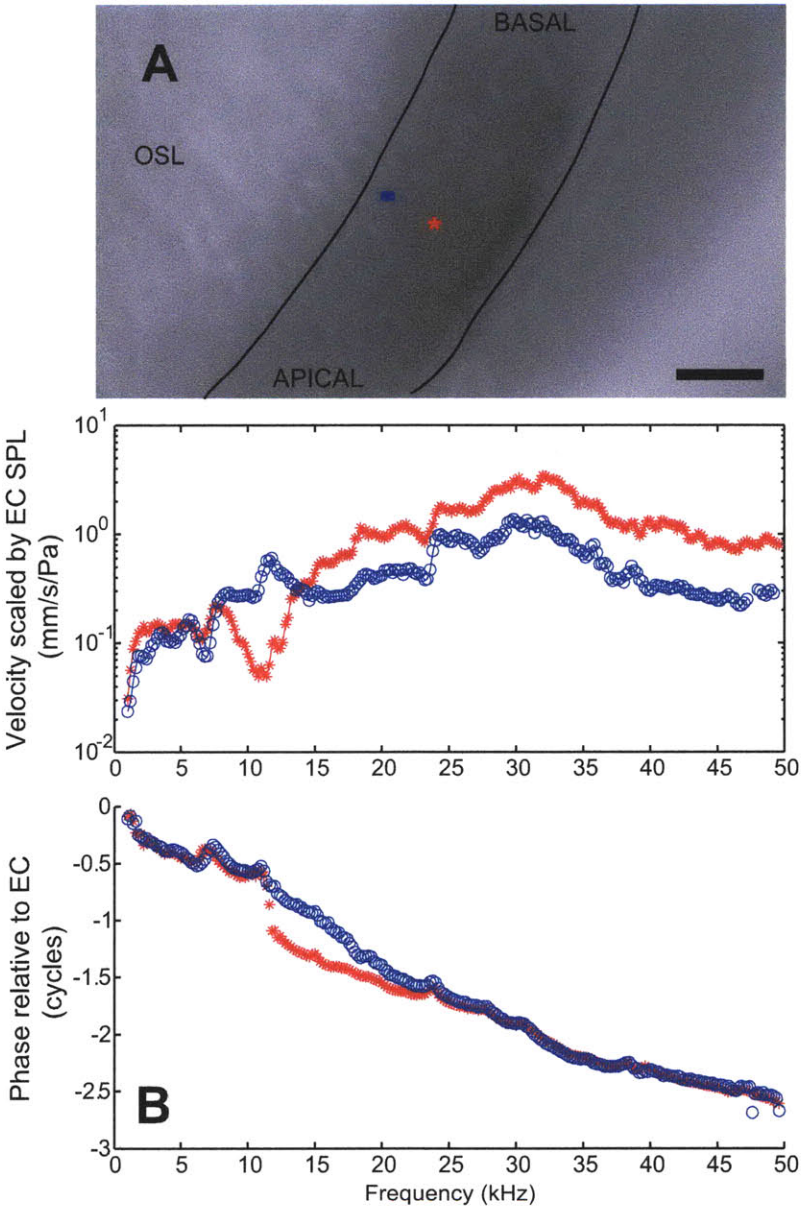

Figure 3-7: In vitro BM responses along the radius of the BM. Panel A shows an image of the gerbil BM with the approximate locations of the beads whose frequency responses are shown in panel B (Scale bar = 100μm). The picture of the BM was taken with an upright microscope at 50X magnification. The BM is outlined with apical and basal directions indicated. OSL = osseous spiral lamina. The magnitude response is given as the velocity in mm/s normalized by the sound pressure in Pascals as measured in the ear canal (EC) with the probe tube microphone. The magnitude responses were smoothed using a three-point mean. The sound pressure delivered to the ear canal was roughly 120 dB SPL. The phase is given as cycles relative to the phase at the EC.

One difficulty in obtaining BM results was the similarity between the responses of beads on torn portions of the transparent RWM and the BM. As shown in figure 3-8, beads that were on the RWM also showed tuning at roughly the same frequency as the BM underneath. In order to determine that these beads were in fact on the RWM, the membrane was mechanically moved with a stainless steel pin, and the beads moved, making it obvious that they were attached to it. We can see that tuning on these beads is not very sharp; however, the bead closer to the center of the BM shows a larger response, similar to what we expect from the responses of beads closer to the center of the BM. We can also see that the magnitude of the responses on the RWM is 100 to 1000$\times$ smaller than the magnitude of responses on the in vivo BM.

3.2 Compound Action Potential

A compound action potential (CAP) measurement was taken before the measurements shown in figures 3-5 and 3-6 were taken. The CAP threshold curve is shown in figure 3-9 and shows that the animal's hearing was poor. The CAP threshold set the minimum sound pressure level at which we were guaranteed to obtain BM motion. This level was roughly 80 dB SPL.

We tried to determine which surgical step caused the greatest threshold increase as measured by CAP and found that upon opening the bulla, the animal's hearing was intact. The majority of damage was caused by removing the round window membrane (RWM) to place reflective beads on the surface of the BM as shown by the data in figure 3-10. Very similar results were obtained in another animal in which CAP was measured before and after removing the RWM.

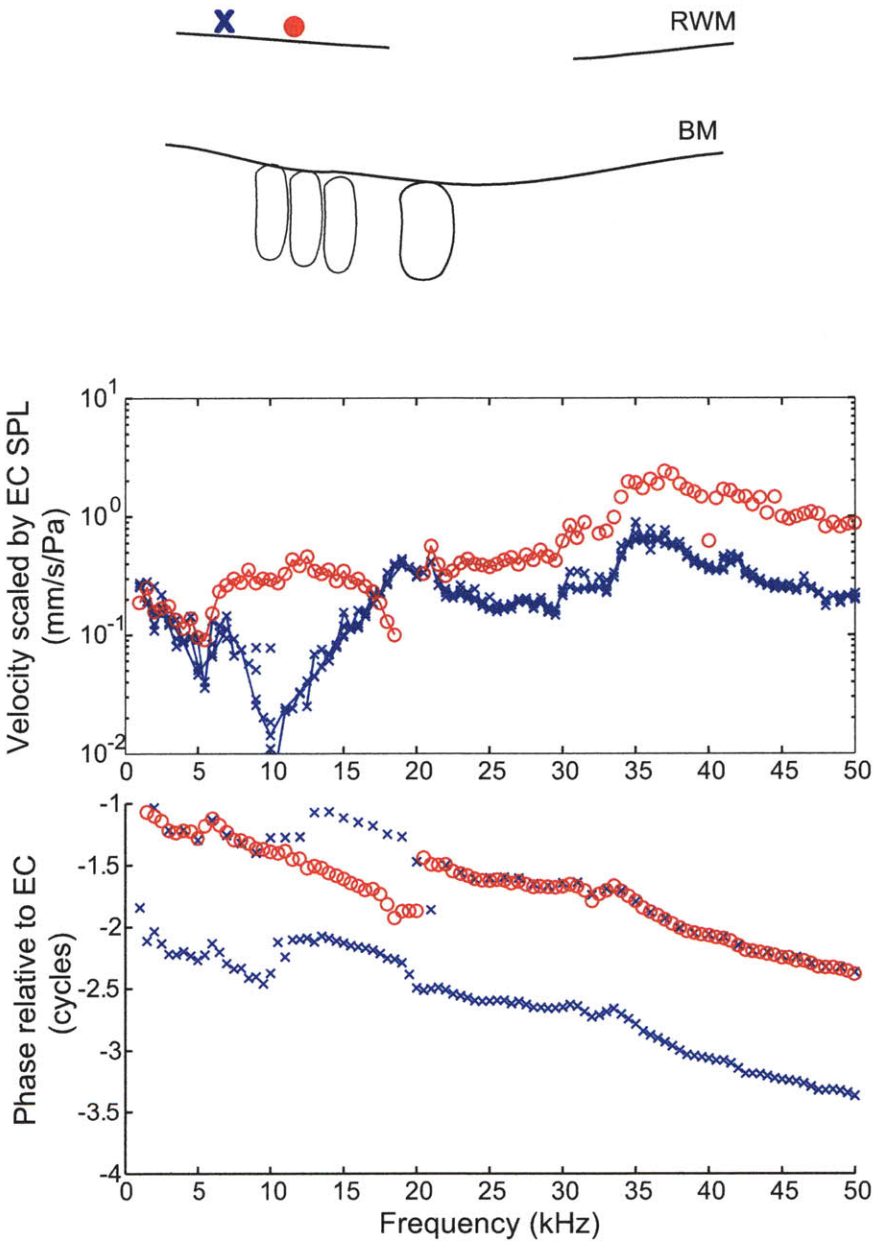

Figure 3-8: Frequency Response of beads on RWM. The two responses shown are of two beads spaced by 20μm on the torn RWM. The exact location of the beads relative to the hair cells is not known. Picture not to scale.

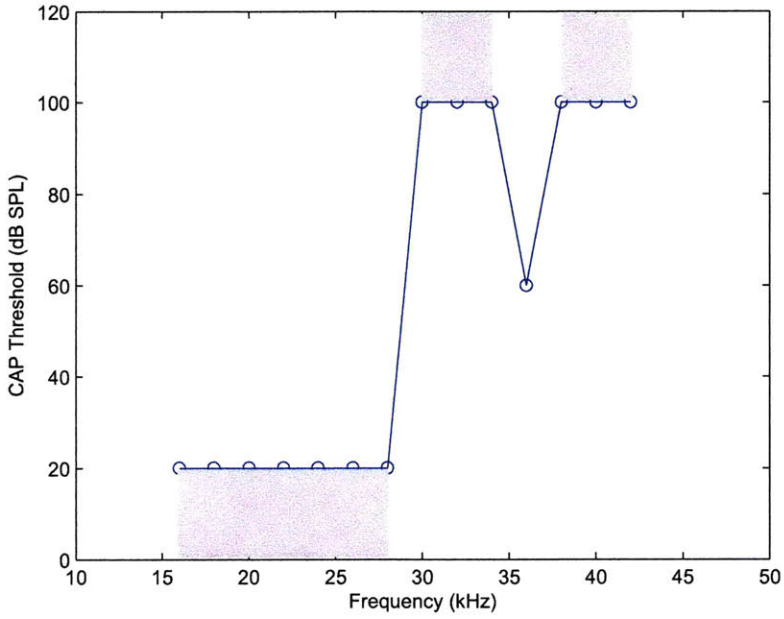

Figure 3-9: CAP measurement for the ear shown in figures 3-5 and 3-6. The minimum sound pressure level attempted was 20 dB SPL, and the maximum attempted was 100 dB SPL as dictated by the probe tube microphone placed in the ear canal. Shading indicates that the CAP threshold was somewhere in the shaded area.

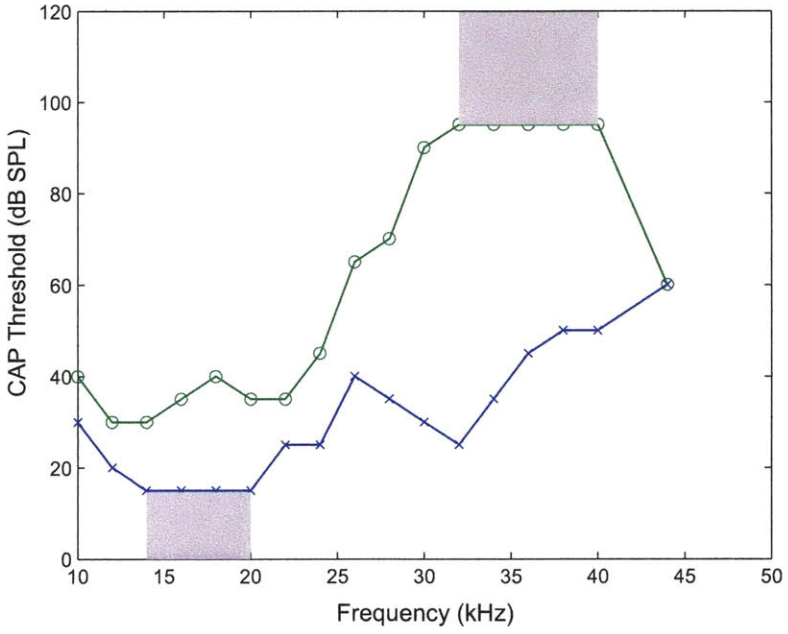

Figure 3-10: CAP measurement before (x) and after (o) removing the RWM to place beads on the BM. The minimum sound pressure level attempted was 15 dB SPL, and the maximum attempted was 95 dB SPL. Shading indicates that the CAP threshold was somewhere in the shaded area.

Chapter 4

Discussion

In this chapter the implications of the results presented in Chapter 3 will be discussed. The aspects of the experimental protocol described in Chapter 2 that were essential to successfully measuring the BM will also be highlighted.

4.1 Validation of Measurements

Looking at the four control measurements outlined in section 3.1.1, we interpret each as follows: 1) looking at our stapes data plotted against that of Ravicz, Cooper, and Rosowski [11], we see similarities between the two responses, i.e. the magnitude and phase have similar slopes (see figure 3-1). Considering that the responses were measured on different animals, with different frequency resolution, and possibly at different angles, the responses can be said to be very similar. 2) Looking at the response of a bead on the BM with sound on and off, we can see that the peak response we measured was not an artifact since the response with no sound was 20 to 60 dB lower than the one with sound and had no significant peak (see figure 3-2). 3) Looking at the effect of using a coverslip on the RW, we saw no significant difference in the major trends of our data when two coverslips were used vs. none. That is, the peak in magnitude was at the same frequency and had the same magnitude, and the phase response showed the same total accumulation (see figure 3-3). 4) Regarding the importance of sealing the ear canal, in one measurement we verified that there was

no significant difference when the EC was sealed vs not (see figure 3-4). This agrees to a certain extent with observations made by de la Rochefoucauld and others in a study measuring the input impedance of the gerbil cochlea [5]. They also observed that sealing the EC had no effect on measurements between 5-50 kHz. We preferred not sealing the EC since heat from our heating pad could melt the Vaseline used to make the seal, causing it to leak into the EC and changing the properties of the ear over time. Further investigation might indicate that sealing the EC is beneficial in which case a sealant with a higher melting point than 38 °C should be used.

In addition to the above mentioned control measurements, we compared our responses to previously published results of gerbil BM motion in the base and found similarities. As shown in figure 3-5, the magnitude response of the same bead measured with the animal alive and dead showed marked differences. The peak response dropped by 20dB, the best frequency (BF) shifted down by one half octave, and the phase response led the live phase response below BF and lagged it above BF. All of these changes upon death agree with the results of Overstreet [10] who has published the only highly sensitive gerbil BM motions in the extreme base of the cochlea.

Regarding the sensitivity of our best response (shown in figure 3-5), we see that the peak response is roughly 34dB above the lowest magnitude part of the response and that the total phase accumulation is 2 cycles. The corresponding values measured in the gerbil base of a cochlea with similar CAP thresholds by de la Rochefoucauld are 35dB and 2 cycles [6]. In addition, de la Rochefoucauld measured points longitudinally away from the stapes and found no significant difference in best frequency until the points were separated by roughly 300μm. Therefore, in figure 3-6 where the two beads on the BM were spaced by 80μm longitudinally, we do not see a difference in BF as expected.

4.2 Radial Modes in Insensitive Cochlea

As shown in figures 3-6, our data of measurements at different radial points along the in vivo BM showed sharper tuning in the center of the BM but similar total phase accumulation. In 3-7, we see no signs of multiple radial modes of motion in the post-mortem BM since the two responses show very similar bandwidths and phase accumulations. Since we have only one in vivo measurement of different spots along the radius of the BM, we need additional data to determine whether or not there could be multiple radial modes of motion in the live cochlea. We must also keep in mind that the in vivo response shown in figure 3-6 is of a cochlea whose CAP thresholds were increased by 40 to 60 dB SPL in the region of interest. Since the responses lacked any sign of non-linearity, they may also be missing other properties associated with a healthy cochlea. We should also note that we were limited to measure spots where our beads happened to fall and thus could not obtain a complete picture of BM motion.

4.3 Stumbling Blocks

4.3.1 Sensitivity of Basilar Membrane Responses

We succeeded in our goal of obtaining in vivo mammalian BM measurements using laser Doppler velocimetry (LDV). However, the results obtained were less sensitive than many previously published results in live animals. In addition, there was no evidence of compressive non-linearity of BM motion with respect to sound pressure level. Among the many possible reasons for insensitive responses is the damage caused to hearing from removing the round window membrane (RWM), a necessary step for allowing beads to settle on the BM and serve as reflective targets. As shown in figure 3-10, CAP thresholds increased by 40 to 50 dB SPL in the frequency region that is easiest to access through the RW due to the step where the RWM was removed. Previous studies have not found this difficulty with removing the RWM in other species. However, in the only published results of BM measurements in the gerbil

through the RWM showing non-linear behavior, the author stated that out of 180 attempts, he was only able to obtain two (2) such results [10]. This indicates that obtaining access to the BM in the base of the gerbil while maintaining healthy hearing is a common difficulty.

Other researchers have had greater success obtaining sensitive gerbil BM responses by accessing more apical regions of the cochlea. This technique requires drilling a hole in the bone surrounding the cochlea which has the potential to cause significant damage [13]. However, it is possible that the lower frequency regions of the gerbil cochlea are less susceptible to the noise damage caused by shaving bone.

An additional cause for CAP threshold increases could have been the fact that the bulla was not heated during the experiment. Although the animal's core temperature was regulated, studies have shown that the bulla temperature can drop significantly due to the invasive surgery and that this can lead to large threshold increases at high frequencies [2]. Therefore, in future studies we intend to maintain the temperature at the bulla using a heating source in a closed loop with a thermocouple placed in or near the round window.

4.3.2 Importance of Bead Properties

One study has shown that gold-coated glass beads of 15 to 25 μm diameter placed on the basal end of the BM follow the motion of the surrounding tissue and that their weight does not affect the sharpness of tuning of the BM or the Compound Action Potential (CAP) [3]. Another study has shown that beads placed on Claudius' cells in the apical region of the cochlea do not follow the motion of the surrounding tissue [8]. Our beads' surfaces were not modified to improve adhesion to the underlying tissue, so at times, beads did move during a measurement. However, most of the beads remained firmly in place after several hours of testing. All of the results presented belong to this group of beads. Several different beads were tested as reflective targets for measuring BM motion using the LDV. In the end the gold-coated polystyrene beads were used because of their combination of high reflectivity, easy availability, and low density.

Coating the beads with gold resulted in a great improvement in our ability to obtain measurements. Although the repeatability of results did not improve significantly, it was much easier to obtain enough reflection off of the beads to make a measurement that could be trusted. Before the beads were coated with gold, it was much more difficult to maintain a reflection signal from the beads.

We also believe that another difficulty in maintaining a good signal on the velocimeter stemmed from the animal's motion caused by breathing. As a partial solution to this problem, a tracheotomy was performed to reduce labored breathing. Another possible solution is to use an anesthetic that suppresses breathing, although this was not tried. However, we did not notice a significant difference in the ability to lock onto a signal on the velocimeter when the animal was dead, suggesting that the problem was not from its breathing. It is possible that a more secure head holder which involves placing screws into the animal's skull then gluing a piece of metal to these screws would reduce motion.

4.3.3 High-Frequency Acoustics

The most challenging aspect of developing the measurement system used for gerbil BM motion was being able to reliably measure sound pressure over the frequencies of interest (1000 to 50000 Hz). As described in section 2.2.1, this problem was finally solved using a probe tube of very small diameter placed very close to the umbo of the ear being measured. Since the tube is so small, any chamber placed next to it behaves as a very low-impedance load. Thus, the size of the cavity used for calibration was not critical.

As an initial attempt to avoid the issue of having to calibrate sound pressure at all frequencies, we tried to measure stapes motion at the end of each experiment and use it as our reference. However, due to the gerbil anatomy, it is difficult to measure the stapes in the same direction as its piston-like motion. Measuring a posterior crus as shown in figure 3-1 is an accepted reference for BM motion but may not give entirely complete results at all frequencies. But the main reason the stapes was not a reliable reference was that sound delivery was not completely repeatable when the animal's

body was moved to gain access to the stapes. Therefore, a reference for sound pressure at the EC at the same time as the BM motion measurement was necessary for stapes measurements as well. In addition, having an accurate measurement of sound pressure in the EC simplified the experiment by reducing the number of measurements.

Chapter 5

Conclusions

In this study, we succeeded in our goal of measuring the motion of the basilar membrane (BM) in a live mammalian cochlea using a laser Doppler velocimeter (LDV). To achieve this goal, we developed the surgical methods required to gain access to the cochlea while keeping the animal alive. We also implemented a system based on the work of Ravicz and others to accurately measure the sound pressure being delivered to the animal's ear canal (EC) using a MEMS microphone coupled to a narrow probe tube [12]. In addition, we developed the software and hardware necessary for delivering sound, measuring responses, and processing data.

We measured the basilar membrane (BM) in the Mongolian gerbil at a distance of roughly 1.5 mm from the extreme base and found a best frequency (BF) of roughly 35 kHz. We chose the base to gain access through the round window membrane (RWM) to minimize the need for invasive surgery. Post-mortem measurements showed a 20dB drop in sensitivity as well as a half-octave drop in BF. The post-mortem phase led the in vivo phase below the BF and lagged the in vivo phase above the BF. These features of the post-mortem response agree with those seen by Overstreet [10] in the base of the gerbil cochlea. To look for evidence of radial modes in the BM, we measured points along the radius of the BM both in vivo and post-mortem. In the in vivo case, we found slightly sharper tuning in the center of the BM than on the edge but similar phase excursions. In the post-mortem case, we found similar bandwidths and phase excursions along the radius of the BM. Since in vivo measurements along the

radius of the BM were only collected in one animal, we cannot yet conclude that there are multiple radial modes in the gerbil BM. In addition, our in vivo preparation was relatively insensitive as evidenced by compound action potential (CAP) thresholds greater than 80dB SPL in the region of interest. We identified the removal of the RWM as the cause for elevated CAP thresholds by comparing the CAP thresholds before and after removing the RWM to drop beads on the BM as essential reflective targets. Previous studies also suggest that large CAP threshold increases are common in the gerbil base ([10], [6]). Similar techniques have led to greater success in larger mammals; however, we hope to apply the lessons learned from measuring the in vivo gerbil cochlea to mice, the only species that would allow us to determine the micromechanical changes underlying genetic hearing disorders.

Bibliography

[1] Leo L. Beranek. *Acoustics.* Acoustical Society of America, 1993.

[2] M. C. Brown, D. I. Smith, and A. L. Nuttall. The temperature dependency of neural and hair cell responses evoked by high frequencies. *J. Acoust. Soc. Am.*, 73:1662–1670, 1983.

[3] N. P. Cooper. Vibration of beads placed on the basilar membrane in the basal turn of the cochlea. *J. Acoust. Soc. Am.*, 106:L59–L64, 1999.

[4] N. P. Cooper and W. S. Rhode. Basilar membrane mechanics in the hook region of cat and guinea-pig cochleae: Sharp tuning and nonlinearity in the absence of baseline position shifts. *Hearing Research*, 63:163–190, 1992.

[5] O. de la Rochefoucauld, W. F. Decraemer, S. M. Khanna, and E. S. Olson. Simultaneous measurements of ossicular velocity and intracochlear pressure leading to the cochlear input impedance in gerbil. *J. Assoc. Res. otolaryngol.*, 9:161–177, 2008.

[6] O. de La Rochefoucauld and E. Olson. The role of organ of corti mass in passive cochlear tuning. *Biophysical Journal*, 93:3434–3450, 2007.

[7] B. M. Johnstone and A. J. Boyle. Basilar membrane vibration examined with the mossbauer technique. *Science*, 158:389–390, 1967.

[8] S. M. Khanna, M Ulfendahl, and C. R. Steele. Vibration of reflective beads placed on the basilar membrane. *Hearing Research*, 116:71–85, 1998.

[9] E. L. LePage. The mammalian cochlear map is optimally warped. *J. Acoust. Soc. Am.*, 114:896–906, 2003.

[10] E. H. Overstreet, A. N. Temchin, and M. A. Ruggero. Basilar membrane vibrations near the round window of the gerbil cochlea. *J. Assoc. Res. otolaryngol.*, 3:351–361, 2002.

[11] M. E. Ravicz, N. P. Cooper, and J. J. Rosowski. Gerbil middle-ear sound transmission from 100 hz to 60 khz. *J. Acoust. Soc. Am.*, 124:363–380, 2008.

[12] M. E. Ravicz, E. S. Olson, and J. J. Rosowski. Sound pressure distribution and power flow within the gerbil ear canal from 100 hz to 80 khz. *J. Acoust. Soc. Am.*, 122:2154–2173, 2007.

[13] T. Ren. Longitudinal pattern of basilar membrane vibration in the sensitive cochlea. *PNAS*, 99:17101–17106, 2002.

[14] L. Robles and M. A. Ruggero. Mechanics of the mammalian cochlea. *Physiology Reviews*, 81:1305–1352, 2001.

[15] M. A Ruggero and N. C Rich. Application of a commercially-manufactured doppler-shift laser velocimeter to the measurement of basilar-membrane vibration. *Hearing Research*, 51:215–230, 1991.

[16] I. J. Russell, P. K. Legan, V. A. Lukashkina, A. N. Lukashkin, R. J. Goodyear, and G. P. Richardson. Sharpened cochlear tuning in a mouse with a genetically modified tectorial membrane. *Nature Neuroscience*, 10:215–223, 2007.

[17] S. M. v. Netten. Laser interferometer microscope for the measurement of nanometer vibrational displacements of a ligh-scattering microscopic object. *J. Acoust. Soc. Am.*, 83:1667–1674, 1988.

[18] G. von Békésy. The vibration of the cochlear partition in anatomical preparations and in models of the inner ear. *J. Acoust. Soc. Am.*, 21:233–245, 1949.